Pushing Raman spectroscopy over the edge: purported signatures of organic molecules in fossil animals are instrumental artefacts

Julien Alleon[1], Gilles Montagnac[2], Bruno Reynard[2], Thibault Brulé[3], Mathieu Thoury[4], Pierre Gueriau[1]*

[1]Institute of Earth Sciences, University of Lausanne, Géopolis, CH-1015 Lausanne, Switzerland.
[2]Université de Lyon, ENS de Lyon, Université Lyon 1, CNRS, LGL-TPE, F-69007 Lyon, France
[3]HORIBA France SAS, 91120 Palaiseau, France
[4]Université Paris-Saclay, CNRS, ministère de la Culture, UVSQ, MNHN, Institut photonique d'analyse non-destructive européen des matériaux anciens, 91192, Saint-Aubin, France
*Corresponding author: pierre.gueriau@hotmail.fr

Abstract

Widespread preservation of fossilized biomolecules in many fossil animals has recently been reported in six studies, based on Raman microspectroscopy. Here, we show that the putative Raman signatures of organic compounds in these fossils are actually instrumental artefacts resulting from intense background luminescence. Raman spectroscopy is based on the detection of photons scattered inelastically by matter upon its interaction with a laser beam. For many natural materials, this interaction also generates a luminescence signal that is often orders of magnitude more intense than the light produced by Raman scattering. Such luminescence, coupled with the transmission properties of the spectrometer, induced quasi-periodic ripples in the measured spectra that have been incorrectly interpreted as Raman signatures of organic molecules. Although several analytical strategies have been developed to overcome this common issue, Raman microspectroscopy as used in the studies questioned here cannot be used to identify fossil biomolecules.

Keywords

Raman, fossil biomolecules, biosignatures, Wavelet transform, Baseline subtraction, edge filter ripples

Introduction

Remnants or derivatives of ancient biomolecules are preserved in exceptional cases in fossils, providing unique information to document the evolutionary history of life during geological time. They can be used, for example, to clarify the phylogenetic affinities of enigmatic fossils[1,2], or to reconstruct the coloration of extinct organisms such as invertebrates, feathered dinosaurs, and mammals[3].

The search for such fossil biomolecules often requires combining as many techniques as available[2]. Fossilized organic pigments were identified using a suite of mass spectroscopy techniques such as gas chromatography-mass spectrometry (GC-MS) and time of flight secondary ion mass spectroscopy (ToF SIMS)[3]. Fourier-transform infrared (FTIR) spectroscopy of 1-billion-year-old microfossils was combined with morphological and ultrastructural observations by transmission electron microscopy (TEM) to interpret them as the earliest fungi[4]. Advanced synchrotron spectroscopic techniques made it possible to highlight that a range of organic (bio)molecules can sometimes experience only partial degradation during diagenesis and even metamorphism, and be identified in various taxa including bacteria, plants and animals[5-14]. Recently, it was suggested that conventional Raman spectroscopy (i.e. equipped with a 532 nm laser as the excitation source under continuous illumination) can be added to the list of techniques previously mentioned, and be used alone to identify organic compounds in fossils[15-20].

In the latter studies, spectroscopic data were interpreted as evidence for the preservation of diverse organic degradation products of biomolecules in more than a hundred different metazoan fossils, such as organic pigments in eumaniraptoran dinosaur eggshells[15] and in a non-avian dinosaur skin[18], as well as of protein, lipid and/or sugar fossilization products in fossil bones[16], dinosaur eggshells[20], and vertebrate and invertebrate soft-tissues[17,19]. Unfortunately, the purported claims of biomolecules in these fossils are not well supported by the data provided, which actually result from instrumental artefacts and data processing. In this paper, we outline the limitations of Raman spectroscopy with respect to the identification of biomolecules in fossil materials, and then describe in detail the origin of the misinterpreted signal.

Raman spectroscopy has important limitations in the study of organic fossils

Raman spectroscopy is widely used in geosciences because it probes the vibration modes of chemical bonds in both solids, liquids, and gases, with minimal sample preparation[21]. Yet, there are several limitations in terms of the sensitivity and accessibility of chemical fingerprints with the technique as used in the studies questioned here. First, excitation with green 514- or 532-nm lasers mostly provides specific information on C-C bonds -- and not about other covalent linkages -- in diagenetically altered organic materials such as fossils[22]. As a result, Raman spectra of organic materials preserved in (meta)sedimentary rocks are dominated by the so-called graphite (G) and defect (D1-D4) bands, which provide information about the structural organization of the aromatic skeleton[23]. Consistently, Raman spectra of geologically altered organic materials can be similar even when they have significantly different elemental and molecular compositions[13,14,24-26]. Second, under continuous illumination, luminescence occurs concurrently with Stokes Raman scattering and generates a signal that overlaps with the Raman spectral window[21,27,28]. Cross sections of Raman (the probability that Raman scattering takes place) are typically 8 to 10 orders of magnitude smaller than that of luminescence. As a result, a number of precautions are often necessary to be able to detect and interpret Raman spectral features among a number of other spectral variations.

The reported periodic broad bands are not Raman signals

In all the studies questioned here[15-20], the spectral bands assigned to organic molecules are broader than the bands usually associated with Raman scattering, and appear quasi-periodic, in contrast to the non-periodic spectral features typically attributed to Raman scattering.

We investigated the periodicity of these bands using wavelet transform (Fig. 1), an effective signal processing technique that is used to decompose a distorted signal into different frequency scales at various resolution levels. Unlike classical Fourier spectral analyses, wavelet transform analyses are advantageous in describing non-stationarities, i.e. localized variations in frequency or magnitude, and providing a direct visualization of the changing statistical properties. It has become a common tool for analysing localized variations within a time series[29,30], but also for spike removal, denoising and background elimination of Raman spectra[31,32]. We selected one spectrum from each of the two studies for which data were made available[15,19]. For

the wavelet analysis displayed in Fig. 1a,b, we selected the spectrum corresponding to the eggshell of the extant flightless bird *Rhea americana*[15], because it is more likely that a pigment is preserved in a modern sample rather than in a fossil. For the wavelet analysis displayed in Fig. 1c,d, we selected the spectrum collected from the crustacean *Acanthotelson stimpsoni* specimen YPM52348[19], because the chitin–protein complex of crustacean cuticles has a high preservation potential[8,33], and this specimen appears to be one of the best preserved (see fig. 1f in [19]) -- the spectrum clearly having been measured from the specimen (unlike for the specimen shown in fig. 1d of [19]). Note that these two spectra, as well as all other reported ones, were provided by the original authors as baseline-subtracted spectra, not as raw data.

Both spectra display numerous broad bands for which our wavelet transform analysis reveals clear high-frequency periodicities of ~64-96 cm^{-1} for wavenumber shifts <1000–1200 cm^{-1}, and of ~128 cm^{-1} for higher wavenumber shifts (Fig. 1a,c). Similar high-frequencies of 130.9 cm^{-1} are obtained by Fast Fourier Transform. Note that the same frequencies are found for all spectra provided by the authors. The 1086 cm^{-1} carbonate Raman peak present in the *R. americana* spectrum reflects the calcified composition of the eggshell, in contrast to all the other (broader) bands, which are best described as a superposition of quasi-periodic wavelets (Fig. 1b,d). These broad, quasi-periodic bands are not the consequence of any Raman effect, but rather result from physical and instrumental artefacts. Indeed, when a sample is illuminated by the laser, the presence of structural defects and inorganic/organic components can generate significant luminescence, often overwhelming the weak Raman signal[21,27]. When this background luminescence is intense, the transmission properties of the interferometric edge filter used to reject the Rayleigh line induce quasi-periodic "ripples" in the measured spectrum[34].

To further illustrate this point, we performed a wavelet analysis on a transmission spectrum of a 532 nm RazorEdge® ultrasteep long-pass edge filter, provided by the manufacturer (Semrock), that is designed to be used as an ultrawide and low-ripple passband edge filter for Raman spectroscopy (Fig. 2). The transmission spectrum of the filter exhibits the aforementioned ripples (Fig. 2a,b). Our wavelet analysis highlights high-frequency periodicities of 64-96 cm^{-1} for low wavenumbers, and of 128 cm^{-1} for higher wavenumbers (Fig. 2b, c), similar to the results reported in the studies questioned herein[15-20]. Such edge filter-related instrumental artefacts

actually explain the presence of most, if not all, of the broad bands that were attributed to organic molecules.

Sample composition does not affect the position of ripples but impacts the shape of the background

The transmission properties of the edge filter induce ripples on the measured spectra when luminescence is intense, making it challenging to identify Raman features without appropriate data processing for background subtraction[34]. The data provided in the publications questioned here[15-20] are only the baseline-subtracted spectra, not the raw data, which makes it impossible to precisely assess the impact of non-Raman processes and sample composition on the corrected spectra from which the presence of organic molecules was inferred. To address these issues, we collected Raman microspectroscopy data on modern and fossil crustaceans in analytical conditions similar to those of the aforementioned studies (for details, see Material and Methods in SI).

We reproduced the experiment performed by McCoy et al.[19] using a specimen of the crustacean *Peachocaris strongi* (Fig. 3a) from the same fossil locality (Mazon Creek, Carboniferous, USA). As with other fossils from Mazon Creek, this specimen is preserved as aluminosilicates and calcite in a sideritic concretion (Fig. S1). In order to further assess the impact of the sample's chemical composition on the measured spectra, we also performed Raman spectroscopy on (i) a specimen of the penaeid shrimp *Cretapenaeus berberus* from the Cretaceous of Morocco (Fig. 3b) preserved as a mixture of calcium phosphates and iron oxides in an illite mudstone (Fig. S1; see also Gueriau et al.[35] and references therein), and (ii) a specimen of the modern shrimp *Neocaridina davidii* (Fig. 3c) dried after death and still rich in organic carbon, likely in the form of chitin (Fig. S1). Whether or not organic carbon is present, and whatever the mineralogical composition of the specimen or its mineral matrix, all the measured spectra (Fig. 3d, solid lines) display broad bands, which all occur at the same wavenumber shifts and add up to a significant background (Fig. 3d, dotted lines). Yet, the shape of the background differs significantly from one measurement to another, and the more intense it is, the more the ripples are expressed. In the baseline-subtracted spectra, the differences in the relative intensity between bands from one measurement to another (Fig. 3e) only result from distinct background profiles of the measurements. A wavelet transform analysis reveals high-frequency periodicities of

64–128 cm^{-1} (Fig. 3f), as was the case for the spectra questioned in the previous section[15-20]. Finally, other than the presence of sharp peaks around 964 and 1086 cm^{-1} (Raman peaks of fluorapatite and calcite, respectively), as well as one unidentified peak at 1156 cm^{-1} in the modern shrimp (possibly carotenoids), which are all three still expressed after subtraction of the frequency components (Fig. 4), spectral differences are limited to relative variations in the ripple band intensity that result from the shape and quality of the baseline fit.

In short, the ripples observed in the Raman microspectroscopy data questioned here represent remnant instrumental signals that result from confounding broad luminescence and inappropriate data processing. The broad luminescence transmitted by the edge filter induced the ripple-shape features above the cut-off wavelength on the raw spectrum. Background correction did not eliminate the ripple-shape distortions induced, and instead accentuated them to give the appearance of putative signatures of organic molecules.

Conclusion and Outlook

Broad bands interpreted to be Raman signatures of diverse organic molecule degradation products in various metazoan fossils[15-20] are artefactual quasi-periodic ripples induced by the edge filter due to intense luminescence, and there is no evidence for Raman signal of organic molecules. Unfortunately, conventional Raman microspectroscopy does not provide direct information on fossil biomolecules[22].

Conventional Raman spectroscopy remains an important paleontological tool providing crucial information on the mineralogical composition of fossils and the degree of crystallization of the carbonaceous remains they preserve, which is often used to quantify the peak temperature organics reached during geological burial[23]. Extracting and interpreting the data, however, requires robust and optimized analytical strategies and/or data processing. Several methods have been developed to remove, *a posteriori,* the undesired contribution of luminescence and ripples in Raman spectra[34,36]. Note that in the papers discussed here[15-20], such processing would leave no signal other than the mineral peaks. Distinct excitation wavelengths, such as near-infrared and ultraviolet, can also be used to significantly limit luminescence[37,38]. Alternatively, non-conventional time-resolved Raman spectroscopy offers new ways to limit or exploit luminescence signals, while techniques based on coherent anti-Stokes Raman scattering (CARS), surface-enhanced Raman spectroscopy (SERS), and

ultraviolet resonance Raman spectroscopy, allow the Raman signal to be considerably enhanced (see Beyssac[27] for review). Furthermore, synchrotron-based X-ray Raman scattering can probe the chemical speciation of light elements such as carbon, in heterogeneous materials usually encountered in life, earth, environmental and materials sciences[39,40].

The search for biomolecules in fossils is a very exciting field of research, offering critical knowledge on both evolutionary events and fossilization processes, yet conventional Raman spectroscopy alone cannot be used to identify fossil biomolecules. Instead, non-conventional Raman spectroscopy, mass spectrometry and infrared and X-ray absorption spectroscopy techniques, are successfully used by paleontologists to identify fossil biomolecules in the geological record[2,41].

Supporting Information

Supporting Information, including details on materials and methods and a supporting figure, is available from the Wiley Online Library or from the author. All data and the R script used in this work are publicly available via the following Dryad Digital Repository: Alleon J, Montagnac G, Reynard B, Brulé T, Thoury M, Gueriau P. 2020. Data from: Pushing Raman spectroscopy over the edge: purported signatures of organic molecules in fossil animals are instrumental artefacts. Dryad Digital Repository: https://doi.org/10.5061/dryad.280gb5mp0 (available upon publication; in the meantime, it can be accessed through the private link below: https://datadryad.org/stash/share/zrJ-IGW9hkU0fjv6BdP5DZsthErRR6UnjUYsj3NA_4w.)

Acknowledgments

We thank Olivier Reubi (UNIL) for his help with Raman spectroscopy, Louise Jensen (EPFL) for her help with scanning electron microscopy, Orla Bath Enright (UNIL) for providing the euthanized specimen of the modern shrimp *Neocaridina davidii.*, and Allison Daley (UNIL) for her English edits and suggestions that helped us improve the clarity of the manuscript. Antoine Pictet (MGL), and Didier Dutheil and Nour-Eddine Jalil (MNHN) provided catalogue numbers for the MGL and MHNM specimens studied herein. We also warmly thank Editor Andrew Moore and two anonymous reviewers for their supportive feedback, suggestions and corrections. This research was conducted in accordance with the University of Lausanne's ethical policy on the use of animals in experiments. This work is a contribution to the Swiss National Science Foundation

project CRSK-2_190580 (PI: P.G.), which funded the research and supported P.G. J.A. was supported by the European Union's Horizon H2020 research and innovation program ERC (STROMATA, grant agreement 759289; PI: Johanna Marin-Carbonne).

ORCIDs

JA, 0000-0002-8286-1976; GM, 0000-0001-9938-0282; BR, 0000-0002-4782-6163; PG, 0000-0002-7529-3456

Conflict of Interest

The authors declare no conflict of interest.

References

[1] Javaux, E. J., Knoll, A. H., & Walter, M. (2003). Recognizing and interpreting the fossils of early eukaryotes. *Origins of Life and Evolution of the Biosphere, 33*(1), 75-94.

[2] Briggs, D. E. G., & Summons, R. E. (2014). Ancient biomolecules: their origins, fossilization, and role in revealing the history of life. *BioEssays, 36*(5), 482-490.

[3] Vinther, J. (2015). A guide to the field of palaeo colour. *BioEssays, 37*(6), 643-656.

[4] Loron, C. C., François, C., Rainbird, R. H., Turner, E. C., Borensztajn, S., & Javaux, E. J. (2019). Early fungi from the Proterozoic era in Arctic Canada. *Nature, 570*(7760), 232-235.

[5] Boyce, C. K., Cody, G. D., Feser, M., Jacobsen, C., Knoll, A. H., & Wirick, S. (2002). Organic chemical differentiation within fossil plant cell walls detected with X-ray spectromicroscopy. *Geology, 30*(11), 1039-1042.

[6] Boyce, C. K., Abrecht, M., Zhou, D., & Gilbert, P. U. P. A. (2010). X-ray photoelectron emission spectromicroscopic analysis of arborescent lycopsid cell wall composition and Carboniferous coal ball preservation. *International Journal of Coal Geology, 83*(2-3), 146-153.

[7] Bernard, S., Benzerara, K., Beyssac, O., Menguy, N., Guyot, F., Brown, G. E., & Goffé, B. (2007). Exceptional preservation of fossil plant spores in high-pressure metamorphic rocks. *Earth and Planetary Science Letters, 262*(1), 257-272.

[8] Cody, G. D., Gupta, N. S., Briggs, D. E. G., Kilcoyne, A. L. D., Summons, R. E., Kenig, F., . . . Scott, A. C. (2011). Molecular signature of chitin-protein complex in Paleozoic arthropods. *Geology, 39*(3), 255-258.

[9] Cosmidis, J., Benzerara, K., Gheerbrant, E., Esteve, I., Bouya, B., & Amaghzaz, M. (2013). Nanometer-scale characterization of exceptionally preserved bacterial fossils in P aleocene phosphorites from O uled A bdoun (Morocco). *Geobiology, 11*(2), 139-153.

[10] Cosmidis, J., Benzerara, K., Menguy, N., & Arning, E. (2013). Microscopy evidence of bacterial microfossils in phosphorite crusts of the Peruvian shelf: Implications for phosphogenesis mechanisms. *Chemical Geology, 359*, 10-22.

[11] Ehrlich, H., Rigby, J. K., Botting, J. P., Tsurkan, M. V., Werner, C., Schwille, P., . . . Sivkov, V. N. (2013). Discovery of 505-million-year old chitin in the basal demosponge Vauxia gracilenta. *Scientific Reports, 3*(1), 1-6.

[12] Wysokowski, M., Zatoń, M., Bazhenov, V. V., Behm, T., Ehrlich, A., Stelling, A. L., . . . Ehrlich, H. (2014). Identification of chitin in 200-million-year-old gastropod egg capsules. *Paleobiology, 40*(4), 529-540.

[13] Alleon, J., Bernard, S., Le Guillou, C., Marin-Carbonne, J., Pont, S., Beyssac, O., . . . Robert, F. (2016). Molecular preservation of 1.88 Ga Gunflint organic microfossils as

a function of temperature and mineralogy. *Nature communications, 7*, 11977. doi: 10.1038/ncomms11977
[14] Alleon, J., Bernard, S., Le Guillou, C., Beyssac, O., Sugitani, K., & Robert, F. (2018). Chemical nature of the 3.4 Ga Strelley Pool microfossils. *Geochemical Perspectives Letters, 7*, 37-42. doi: 10.7185/geochemlet.1817
[15] Wiemann, J., Yang, T.-R., & Norell, M. A. (2018). Dinosaur egg colour had a single evolutionary origin. *Nature, 563*(7732), 555-558.
[16] Wiemann, J., Fabbri, M., Yang, T.-R., Stein, K., Sander, P. M., Norell, M. A., & Briggs, D. E. G. (2018). Fossilization transforms vertebrate hard tissue proteins into N-heterocyclic polymers. *Nature communications, 9*(1), 1-9.
[17] Wiemann, J., Crawford, J. M., & Briggs, D. E. G. (2020). Phylogenetic and physiological signals in metazoan fossil biomolecules. *Science Advances, 6*(28), eaba6883.
[18] Fabbri, M., Wiemann, J., Manucci, F., & Briggs, D. E. G. (2020). Three-dimensional soft tissue preservation revealed in the skin of a non-avian dinosaur. *Palaeontology, 63*(2), 185-193.
[19] McCoy, V. E., Wiemann, J., Lamsdell, J. C., Whalen, C. D., Lidgard, S., Mayer, P., . . . Briggs, D. E. G. (2020). Chemical signatures of soft tissues distinguish between vertebrates and invertebrates from the Carboniferous Mazon Creek Lagerstätte of Illinois. *Geobiology*.
[20] Norell, M. A., Wiemann, J., Fabbri, M., Yu, C., Marsicano, C. A., Moore-Nall, A., . . . Zelenitsky, D. K. (2020). The first dinosaur egg was soft. *Nature, 583*, 406–410.
[21] Pasteris, J. D., & Beyssac, O. (2020). Welcome to Raman spectroscopy: successes, challenges, and pitfalls. *Elements, 16*(2), 87-92.
[22] Pasteris, J. D., & Wopenka, B. (2003). Necessary, but not sufficient: Raman identification of disordered carbon as a signature of ancient life. *Astrobiology, 3*(4), 727-738.
[23] Beyssac, O., & Lazzeri, M. (2012). Application of Raman spectroscopy to the study of graphitic carbons in the Earth Sciences. Applications of Raman spectroscopy to Earth sciences and cultural heritage. *EMU Notes in Mineralogy, 12*, 415-454.
[24] Quirico, E., Montagnac, G., Rouzaud, J.-N., Bonal, L., Bourot-Denise, M., Duber, S., & Reynard, B. (2009). Precursor and metamorphic condition effects on Raman spectra of poorly ordered carbonaceous matter in chondrites and coals. *Earth and Planetary Science Letters, 287*(1-2), 185-193.
[25] Bernard, S., Horsfield, B., Schulz, H.-M., Schreiber, A., Wirth, R., Vu, T. T. A., . . . Sherwood, N. (2010). Multi-scale detection of organic and inorganic signatures provides insights into gas shale properties and evolution. *Chemie der Erde, 70*, 119-133.
[26] Alleon, J., Flannery, D. T., Ferralis, N., Williford, K. H., Zhang, Y., Schuessler, J. A., & Summons, R. E. (2019). Organo-mineral associations in chert of the 3.5 Ga Mount Ada Basalt raise questions about the origin of organic matter in Paleoarchean hydrothermally influenced sediments. *Scientific Reports, 9*, 1-13.
[27] Beyssac, O. (2020). New trends in Raman spectroscopy: from high-resolution geochemistry to planetary exploration. *Elements, 16*(2), 117-122.
[28] Pucéat, E., Reynard, B., & Lécuyer, C. (2004). Can crystallinity be used to determine the degree of chemical alteration of biogenic apatites? *Chemical Geology, 205*(1-2), 83-97.
[29] Torrence, C., & Compo, G. P. (1998). A practical guide to wavelet analysis. *Bulletin of the American Meteorological Society, 79*(1), 61-78.
[30] Debret, M., Bout-Roumazeilles, V., Grousset, F., Desmet, M., McManus, J. F., Massei, N., . . . Trentesaux, A. (2007). The origin of the 1500-year climate cycles in Holocene North-Atlantic records.
[31] Ehrentreich, F., & Sümmchen, L. (2001). Spike removal and denoising of Raman spectra by wavelet transform methods. *Analytical Chemistry, 73*(17), 4364-4373.

[32] Hu, Y., Jiang, T., Shen, A., Li, W., Wang, X., & Hu, J. (2007). A background elimination method based on wavelet transform for Raman spectra. *Chemometrics and Intelligent Laboratory Systems, 85*(1), 94-101.
[33] Stankiewicz, B. A., Mastalerz, M., Hof, C. H. J., Bierstedt, A., Flannery, M. B., Briggs, D. E. G., & Evershed, R. P. (1998). Biodegradation of the chitin-protein complex in crustacean cuticle. *Organic Geochemistry, 28*(1-2), 67-76.
[34] Casadio, F., Daher, C., & Bellot-Gurlet, L. (2017). Raman spectroscopy of cultural heritage materials: overview of applications and new frontiers in instrumentation, sampling modalities, and data processing *Analytical Chemistry for Cultural Heritage* (pp. 161-211): Topics in Current Chemistry Collections. Springer.
[35] Gueriau, P., Bernard, S., Farges, F., Mocuta, C., Dutheil, D. B., Adatte, T., . . . Charbonnier, S. (2020). Oxidative conditions can lead to exceptional preservation through phosphatization. *Geology*.
[36] Sanz-Arranz, A., Manrique-Martinez, J. A., Medina-Garcia, J., & Rull-Perez, F. (2017). Amorphous zinc borate as a simple standard for baseline correction in Raman spectra. *Journal of Raman Spectroscopy, 48*(11), 1644-1653.
[37] Quirico, E., Bonal, L., Montagnac, G., Beck, P., & Reynard, B. (2020). New insights into the structure and formation of coals, terrestrial and extraterrestrial kerogens from resonant UV Raman spectroscopy. *Geochimica et Cosmochimica Acta, 282*, 156-176.
[38] Jehlička, J., Edwards, H. G. M., & Vítek, P. (2009). Assessment of Raman spectroscopy as a tool for the non-destructive identification of organic minerals and biomolecules for Mars studies. *Planetary and space Science, 57*(5-6), 606-613.
[39] Gueriau, P., Rueff, J.-P., Bernard, S., Kaddissy, J. A., Goler, S., Sahle, C. J., . . . Bergmann, U. (2017). Noninvasive synchrotron-based X-ray Raman scattering discriminates carbonaceous compounds in ancient and historical materials. *Analytical chemistry, 89*(20), 10819-10826.
[40] Georgiou, R., Gueriau, P., Sahle, C. J., Bernard, S., Mirone, A., Garrouste, R., . . . Bertrand, L. (2019). Carbon speciation in organic fossils using 2D to 3D x-ray Raman multispectral imaging. *Science Advances, 5*(8), eaaw5019.
[41] Alleon, J., & Summons, R. E. (2019). Organic geochemical approaches to understanding early life. *Free Radical Biology and Medicine, 140*, 103-112.

Figure captions

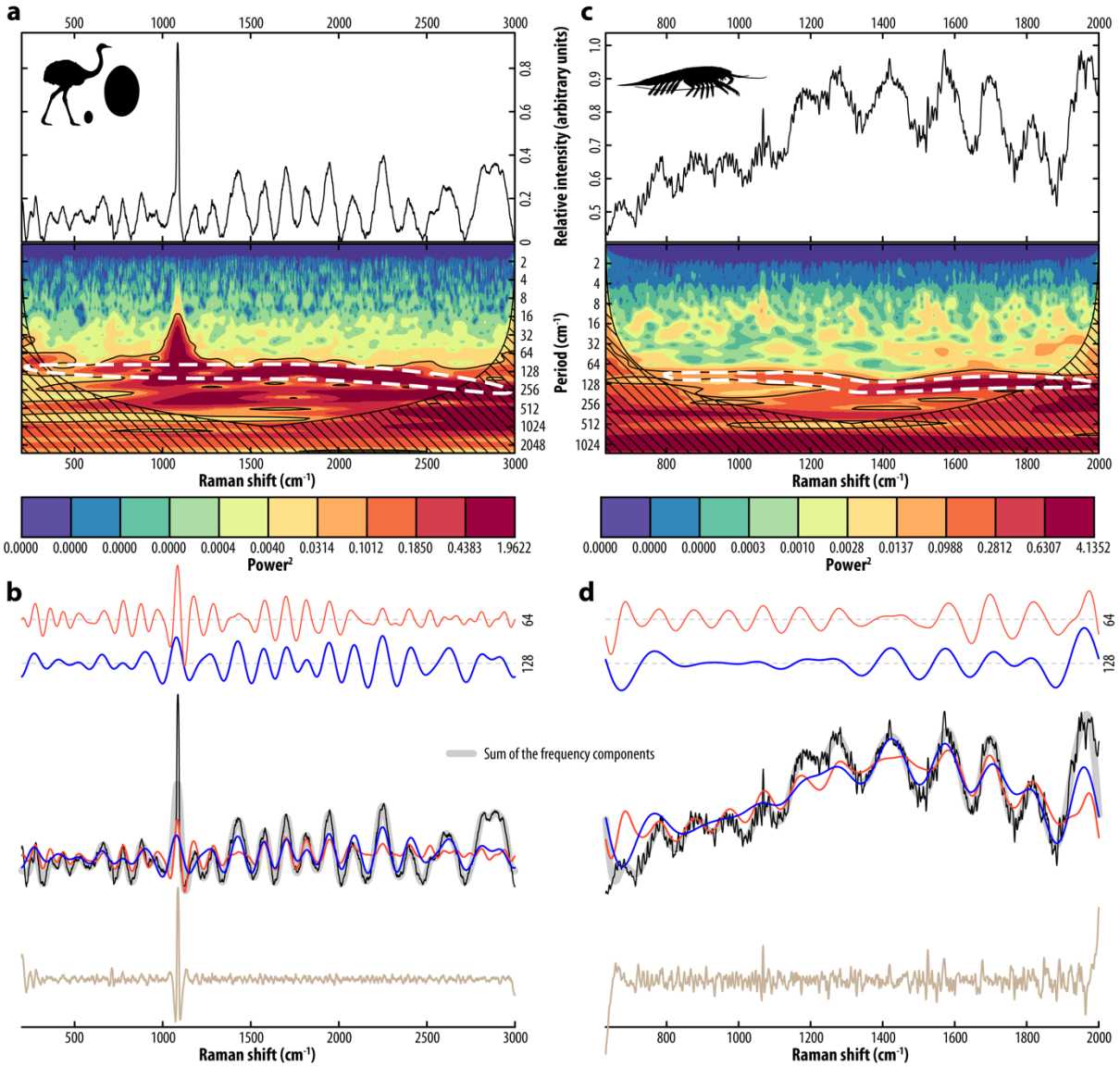

Figure 1. Periodic wavelet analysis of Raman spectra from the eggshell of the extant flightless bird *Rhea americana* (a,b; data from [15]), and from the Carboniferous crustacean *Acanthotelson stimpsoni* specimen YPM52348 (c,d; data from [19]). The hatched area marks parts of the spectrum where energy bands are likely to appear less powerful than they actually are. **a,c)** Baseline-subtracted spectra and their wavelet transform analysis show a clear high-frequency periodicity of 64–128 cm^{-1}. **b,d)** 64 and 128 cm^{-1} frequency components extracted from a wavelet multiresolution analysis (top, in red and blue, respectively) and superimposed, together with the sum of all frequency components, on the spectra. For clarity, the residuals after frequency subtraction are shifted down along the vertical axis.

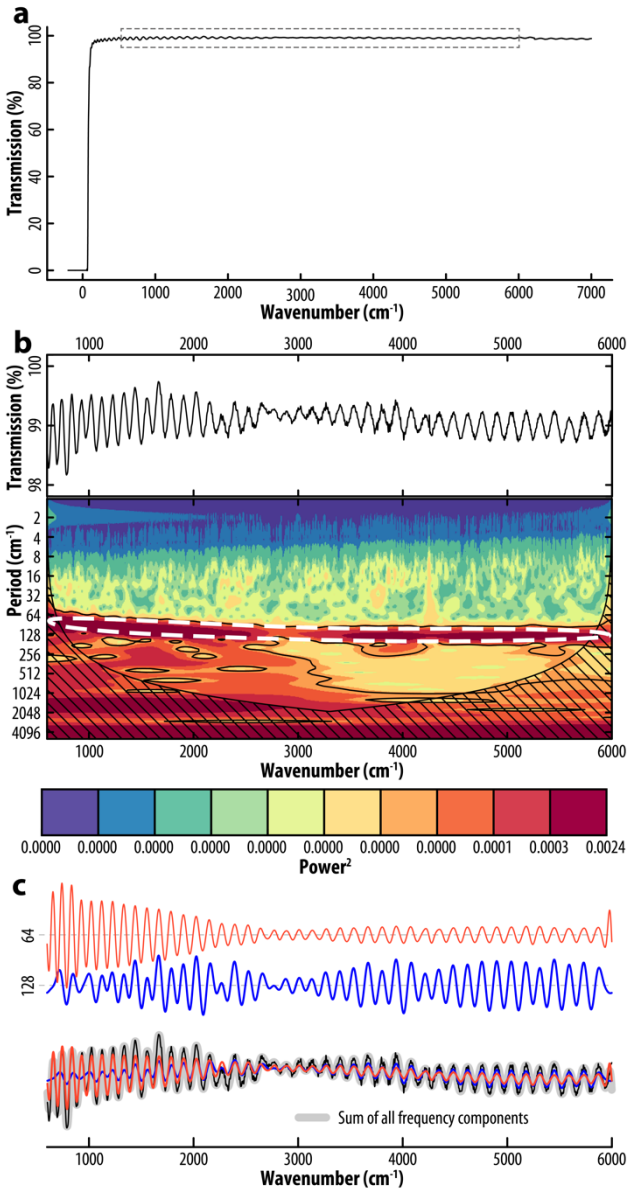

Figure 2. Wavelet transform analysis of the transmission spectrum of a 532 nm RazorEdge® ultrasteep long-pass edge filter (Semrock). **a)** Transmission spectrum of the edge filter between -200 and 7000 cm^{-1}. **b)** Wavelet transform analysis of the spectrum between 600 and 6000 cm^{-1} (rectangle in a) showing a clear high-frequency periodicity of 64–128 cm^{-1}. **c)** 64 and 128 cm^{-1} frequency components extracted from a wavelet multiresolution analysis (top, in red and blue, respectively) and superimposed, together with the sum of all frequency components, on the spectrum.

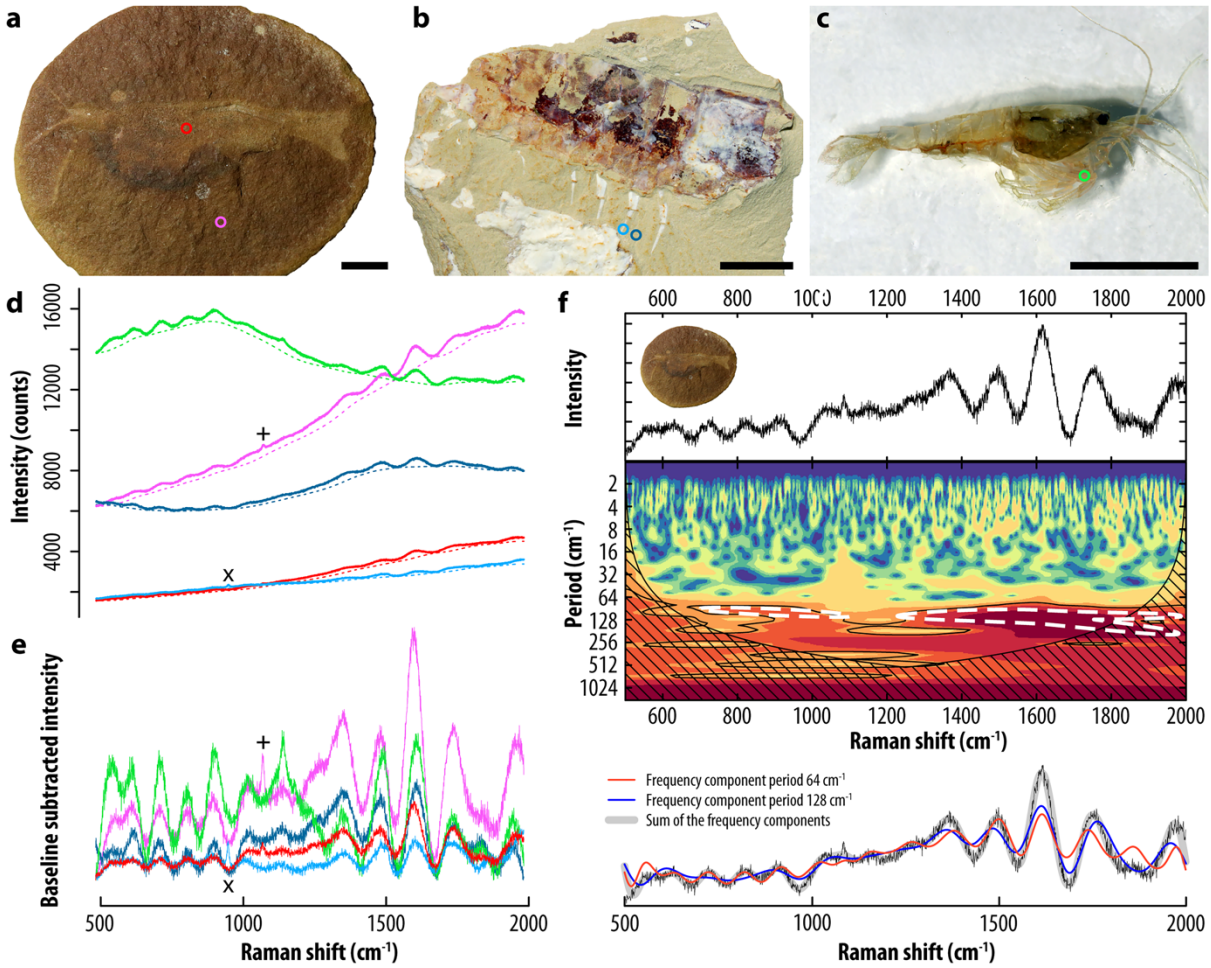

Figure 3. Raman spectroscopic data of fossil and modern shrimps of different chemistry. **a–c)** Photographs of the Carboniferous shrimp *Peachocaris strongi* from Mazon Creek, USA [specimen MGL.107330] (a), the Cretaceous penaeid shrimp *Cretapenaeus berberus* from OT1, Morocco [specimen MHNM-KK-OT 52a] (b), and the extant shrimp *Neocaridina davidii* dried (c). **d)** Raw spectra collected from the areas identified by circles in a–c (solid line), and their baseline (dotted line) as modeled in Spectragryph 1.2 using a 15% adaptive baseline; **e)** corresponding baseline-subtracted spectra. Nearly all bands account for instrumental artefact due to non-linear transmission of the edge filter. Only the sharp peaks highlighted by × and + around 964 and 1086 cm^{-1} (fluorapatite and calcite peaks, respectively) in d and e represent Raman signal. **f)** Wavelet transform analysis of the spectrum collected from *P. strongi* (red in e) showing a high-frequency periodicity between 64 and 128 cm^{-1}. Scale bars represent 5 mm.

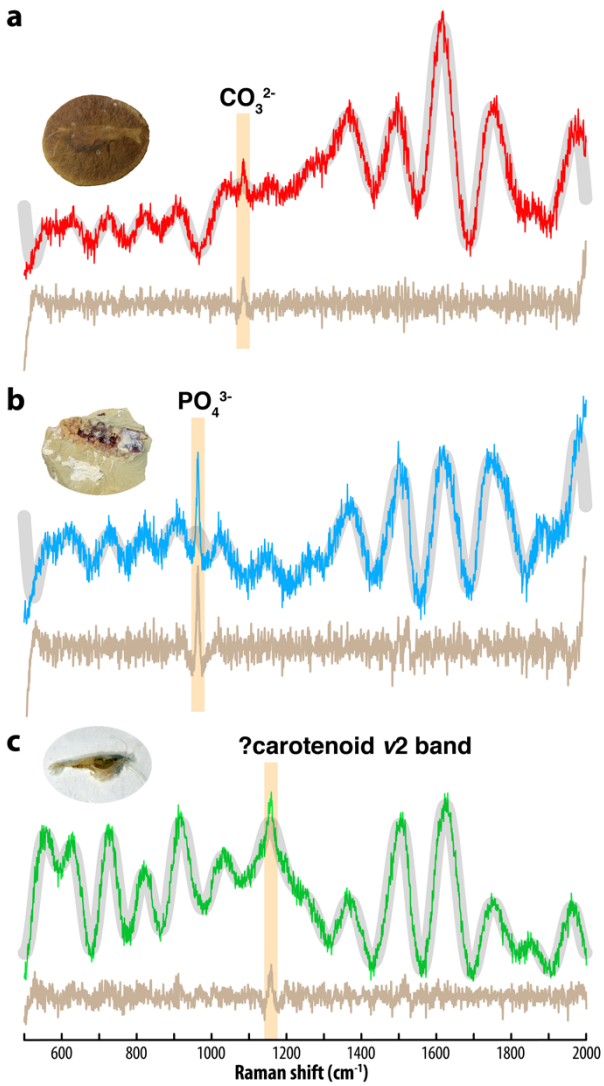

Figure 4. Raman peaks still expressed after subtraction of the frequency components. **a–c)** Baseline-subtracted spectra (color), sum of all frequency components (gray) and residuals after frequency subtraction (light brown) for the Carboniferous shrimp *Peachocaris strongi* from Mazon Creek, USA [specimen MGL.107330] (a), the Cretaceous penaeid shrimp *Cretapenaeus berberus* from OT1, Morocco [specimen MHNM-KK-OT 52a] (b), and the extant shrimp *Neocaridina davidii* dried (c). For clarity, the residuals are shifted down along the vertical axis.